Advanced Ceramics Progress: Vol. 10, No. 3, (Summer 2024) 1-7

Materials and Energy Research Center
MERC

Contents lists available at ACERP

Advanced Ceramics Progress

Journal Homepage: www.acerp.ir

Original Research Article

Microstructure and Properties of Spark Plasma Sintered SiAlON Composites Derived from Novel Precursors

Mohammad Sadegh Abdi Maghsoudlou [a,b*], Touradj Ebadzadeh [c], Alireza Aghaei [d]

[a] *Assistant professor , Department of Materials Engineering,Facalty of Engineering, Malayer University, Malayer, Iran.*
[b] *PhD Candidate, Department of Ceramics, Materials and Energy Research Center, Karaj, Iran.*
[c] *Professor, Department of Ceramics, Materials and Energy Research Center, Karaj, Iran.*
[d] *Associate Professor, Department of Ceramics, Materials and Energy Research Center, Karaj, Iran.*
*Corresponding Author Email: msabdi@malayeru.ac.ir, msabdim@gmail.com (M.S. Abdi Maghsoudlou) URL: https://www.acerp.ir/article_211749.html

ARTICLE INFO

Article History:
Received: 05 November 2024
Revised: 22 November 2024
Accepted: 23 November 2024

Keywords:
SiAlON Composites,
Novel Precursors,
Spark Plasma Sintering,
Carbothermal Reduction and Nitridation Process,
Mechanical Properties

ABSTRACT

This paper explores α/β-SiAlON composites, known for their exceptional mechanical and thermal properties, fabricated using spark plasma sintering (SPS). Novel reagents were initially introduced for the mechanochemical synthesis of precursors essential for producing α- and β-SiAlON phases via the carbothermal process. The prepared precursors were combined with active carbon in stoichiometric ratios and heated in a nitrogen (N_2) atmosphere for two hours. Characterization techniques, including X-ray diffraction (XRD), Fourier-transform infrared spectroscopy (FTIR), and field emission scanning electron microscopy (FE-SEM), confirmed the successful synthesis of SiAlON phases at 1500°C, revealing a range of morphologies.The results demonstrate that all composites sintered through the SPS process achieve complete densification at 1800°C. Mechanical properties, such as hardness and fracture toughness, are influenced by the ratios of α- and β-SiAlON phases. A composition of 70% β-SiAlON and 30% α-SiAlON exhibited optimal results, achieving a fracture toughness of 4.67 MPa•$m^{1/2}$ and a hardness of 17.32 GPa, comparable to commercial samples produced using alternative raw materials.

https://doi.org/10.30501/acp.2024.486092.1170

1. INTRODUCTION

SiAlON ceramics are solid solutions composed of four abundant elements: silicon (Si), aluminum (Al), oxygen (O), and nitrogen (N)(Nag et al., 2021; Ogunbiyi et al., 2024). These ceramics are highly regarded for their impressive strength and durability, enabling them to withstand extreme temperatures and harsh environmental conditions. Consequently, SiAlON-based ceramics are well-suited for a wide range of industrial applications, including cutting tools, bearings, metal forming, and molten metal handling (Basu et al., 2003; Nag et al., 2021). Several types of SiAlON compounds exist, including β-SiAlON, α-SiAlON, O-SiAlON, and x-SiAlON (Bagci et al., 2023; Ogunbiyi et al., 2024). Due to their exceptional thermal stability, mechanical strength, and chemical resistance, the β and α-SiAlON phases are considered superior to the others. β-SiAlON is known for its high strength and fracture toughness, while α-SiAlON offers excellent wear and oxidation resistance (D. Liu et al., 2024). Despite the appealing properties of SiAlON ceramics, their fracture toughness remains relatively low (3–8 MPa), and these composites do not exhibit an R-curve. These limitations hinder the widespread application of these materials and reduce their reliability across various industries (Kruzic et al., 2008; Kumar et al., 2009). An effective strategy to

Please cite this article as: Abdi Maghsoudlou, M. S., Ebadzadeh, T. & Aghaei, A. (2024). Microstructure and Properties of Spark Plasma Sintered SiAlON Composites Derived from Novel Precursors, *Advanced Ceramics Progress*, 10(3), 1-7. https://doi.org/10.30501/acp.2024.486092.1170

2423-7485/© 2024 The Author(s). Published by MERC.
This is an open access article under the CC BY license (https://creativecommons.org/licenses/by/4.0/).

improve these properties is to develop composites by integrating SiAlON phases with nitride compounds or advanced materials such as SiC, ZrO_2, graphite, and $MoSi_2$. Blending SiAlON powders with nitride compounds leverages their compatible Young's moduli and elastic strains, similar thermal expansion coefficients, and chemical compatibility between the matrix and the reinforcing phase (Sopicka-Lizer et al., 2013; Xu et al., 2015). This approach consequently enhances key properties such as hardness, flexural strength, and toughness in the final composite (α + β) (Guo et al., 2022; Jones et al., 2003). SiAlON composites can be produced using two primary methods with various raw materials. The first method is reaction sintering, which can be carried out using techniques such as spark plasma sintering (SPS)(L. Liu et al., 2011; Nekouee & Khosroshahi, 2016), hot pressing (McGarrity et al., 2024), and gas pressure sintering (GPS) (Ogunbiyi et al., 2024). The second method involves synthesizing each phase separately using different techniques, such as carbothermal synthesis (CS) (Abdi Maghsoudlou et al., 2022; MacKenzie & Barneveld, 2006) or self-propagating high-temperature synthesis (SHS) (Kheirandish et al., 2016; H. C. Yi & Moore, 1990). After synthesizing the desired phases, the resulting powders are mechanically mixed in varying ratios and converted into composite materials by heating at high temperatures. Although the second method consists of two stages—synthesis followed by the production of composite materials through high-temperature heating—it offers greater control over phase ratios and the proportions of both crystalline and glassy phases compared to the first method. As a consolidation method, Spark Plasma Sintering (SPS) has gained popularity among researchers for synthesizing and sintering advanced materials, particularly Si_3N_4-based ceramics. SPS is a pressure-assisted sintering system that allows very rapid heating and cooling, resulting in the production of nearly fully dense materials with a fine-grained microstructure. This process occurs at lower temperatures and in shorter times compared to conventional hot pressing. Research on the synthesis and sintering of SiAlON ceramics using SPS has demonstrated its capability to produce dense SiAlON compounds at lower temperatures from either commercial powders or mechanically activated powder mixtures. Research indicates that SPS is effective in synthesizing and sintering SiAlON ceramics from commercial powders or mechanically activated powder mixtures, achieving high density at reduced temperatures. In this regard, this method can be proposed as a promising solution to producing advanced materials due to its efficiency (Abdi Maghsoudlou et al., 2022).

In this study, novel reagents were developed for the mechanochemical synthesis of precursors essential for producing α and β-SiAlON phases. Initially, fine and pure α and β-SiAlON powders were synthesized separately using a carbothermal reduction and nitridation (CRN) process. After characterization, these synthesized SiAlON powders served as raw materials for producing SiAlON composites. Consequently, the microstructure, sintering characteristics, and mechanical properties of the α/β-SiAlON composites fabricated through the spark plasma sintering (SPS) method were reported for the first time.

2. MATERIALS AND METHODS

All raw materials used in this research for synthesizing the precursors include Aluminum Chloride hexahydrate ($AlCl_3.6H_2O$; 99.9% purity, Merck, Germany), Sodium Metasilicate nonahydrate ($Na_2SiO_3.9H_2O$; GR grade, 99.9% purity, Shantou Xilong Chemical Co., China), Calcium Chloride dihydrate ($CaCl_2.2H_2O$), Ammonium Chloride (NH_4Cl; 99.9% purity, Merck, Germany), and activated Carbon (extra pure, Merck, Germany). According to (Abdi Maghsoudlou et al., 2022), the starting reagents were manually combined in stoichiometric molar ratios for β-$Si_4Al_2O_4N_6$ (z=2) and α-$CaSi_9Al_3N_{15}$. To prepare the precursor for $Si_4Al_2O_4N_6$ (z=2), $AlCl_3.6H_2O$, $Na_2SiO_3.9H_2O$, and NH_4Cl were mixed in stoichiometric ratios of 2:4:2, respectively.

The precursor for α-$CaSi_9Al_3N_{15}$ was obtained by blending $CaCl_2.2H_2O$, $AlCl_3.6H_2O$, NH_4Cl, and $Na_2SiO_3.9H_2O$ in a stoichiometric ratio of 1:3:7:9, respectively. The mixtures were then placed in a Zirconia jar and subjected to high-energy milling using a Retsch planetary ball mill (type PM 400) for approximately 15 minutes, utilizing 250 ml Zirconia jars and 15 Zirconia balls (15 mm diameter) as milling media. The rotation speed and ball-to-powder mass ratio were set at 250 rpm and 10:1, respectively.

After the mechanochemical process, the milled powders were washed multiple times with distilled water to remove soluble salts, dried at 100°C, and then manually mixed with activated carbon in stoichiometric ratios (Abdi Maghsoudlou et al., 2022). This mixture was dispersed in ethyl alcohol in a plastic bottle and ball-milled using a conventional batch-type ball mill for 2 hours. After drying, the resulting powders were uniaxially dry-pressed at 20 MPa and placed in an alumina boat. They were heated to 1500°C to synthesize SiAlON powders. This process was conducted in the alumina boat at a heating rate of 10°C/min for 2 hours in an electric tube furnace under a high-purity nitrogen atmosphere. To eliminate residual carbon, the as-

synthesized powders were burned in air at 700°C for 2 hours.

The phases developed during heating were examined using X-ray diffraction (X'Pert Pro MPD, Panalytical) with CuKα radiation (λ = 0.154 nm) over a 2θ range of 10–80 degrees. Fourier transform infrared spectroscopy (RXI spectrometer, Perkin Elmer) recorded FTIR spectra of synthesized SiAlON powders in the wavenumber range of 400–4000 cm^{-1}. The morphology and elemental composition of the obtained SiAlON powders and the microstructure of the sintered samples were inspected using field emission scanning electron microscopy (FESEM, Tescan, Mira3). Prior to FESEM observation, the microstructure of sintered samples was etched using a melt bath of (90% KNO_3 + 10% KOH) at 485°C for 15 minutes.

To create composites, the prepared powders were mixed in varying ratios and blended using the SPEX Mixer (Mill 8000) for 15 minutes. The mixed powders were loaded into a cylindrical graphite die and sintered using the SPS technique at 1800°C with a soaking time of 20 minutes in a vacuum atmosphere. The SPS process was performed in a cylindrical graphite die with a 20 mm inner diameter, applying high pulsed direct current and a pressure of 50 MPa during the sintering cycle. The bulk density and porosity of the sintered specimens were determined using Archimedes' method (ASTM C373-88). Additionally, the microhardness (Hv) of the sintered samples was measured through a Vickers microhardness tester (MKV-h21) under a load of 10 kg for 10 seconds, with at least five successive indentations for each specimen. Fracture toughness was evaluated using the indentation test proposed by Evans et al., with values calculated according to equation (1) (Jones et al., 2003).

$$((K_{IC}.\square)/Hv.(\square)^{1/2}) = 0.15k(c/\square)^{-3/2} \quad (1)$$

where K_{IC} represents the fracture toughness measured in $MPa.m^{1/2}$. The constant Φ is set at 3 while Hv denotes the Vickers microhardness. The correction factor k is 3.2, specifically applicable for high c/α values. The variable c indicates the mean length of the crack (in meters), and α stands for half of the horizontal length of the diagonal (in meters)(Jones et al., 2003).

3. RESULTS AND DISCUSSION

The carbothermal reduction and nitridation (CRN) process performed on two SiAlON precursors, α and β, is illustrated in Figure 1. The X-ray diffraction (XRD) patterns reveal that the precursors, prepared through mechanical activation, transform into pure α- and β-SiAlON powders after being heated at 1500°C for 2 hours. As shown in Figure 1(a), the primary SiAlON phase identified is β-$Si_4Al_2O_2N_6$, accompanied by the formation of β-$Si_2Al_4O_4N_4$ and Al_2O_3. Figure 1(b) indicates that the main phase obtained from the second precursor is α-$CaSi_9Al_3N_{15}$, with some β-SiAlON crystallizing as a secondary phase alongside α-SiAlON.

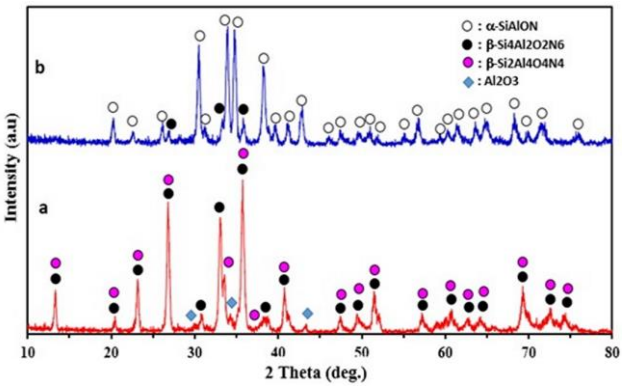

Figure 1. XRD patterns of powders synthesized at 1500°C for 2 hours (a) □-SiAlON (b) □-SiAlON.

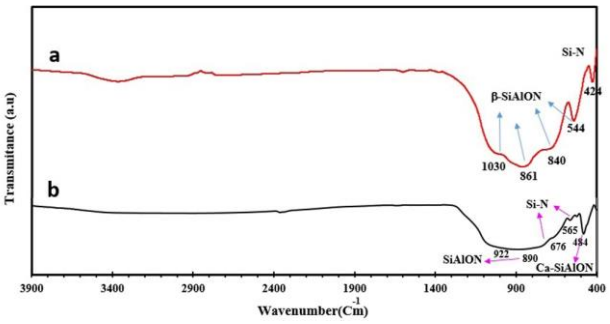

Figure 2. FTIR spectra of the SiAlON compounds prepared at 1500°C for 2 hours (a) □-SiAlON (b) □-SiAlON.

The Fourier-transform infrared (FTIR) spectra of the synthesized SiAlON compounds are presented in Figure 2. The absorption peaks at 424, 544, 690, 854, and 1040 cm^{-1} in the FTIR spectrum (Fig. 2(a)) are attributed to the oxynitride phase, such as β-SiAlON (Antsiferov et al., 2002). Additionally, the peaks at 484, 525, and 565 cm^{-1} in the FTIR spectrum (Fig. 2(b)) confirm the formation of the α-SiAlON phase in the processed precursor at 1500°C (Antsiferov et al., 2002). The FTIR data in Figure 2 align with the XRD results, indicating that nitrogen gas diffuses into the precursors at high temperatures, reacts with various compounds, and facilitates the formation of the desired phases during the CRN process. These findings suggest that the novel reagents used in this study have significant potential for synthesizing SiAlON phases, despite the complexity involved in the SiAlON formation process.

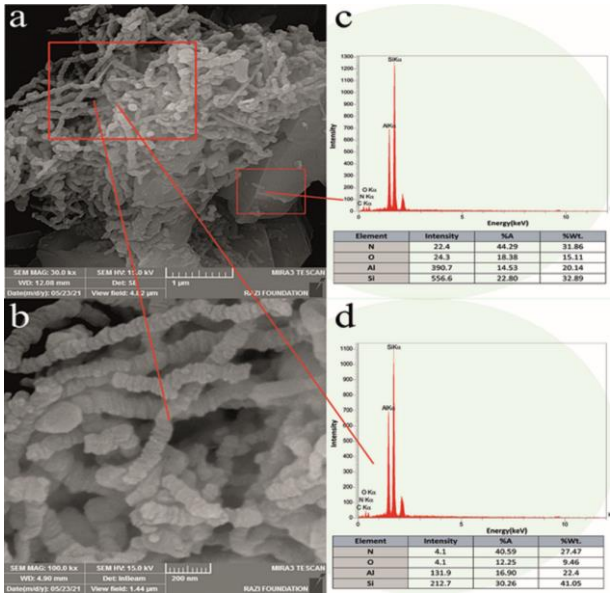

Figure 3. The morphology and chemical composition of the β-SiAlON powder obtained at 1500°C.

The morphology and chemical composition of the β-SiAlON powder, examined using field emission scanning electron microscopy (FE-SEM), are displayed in Figure 3.

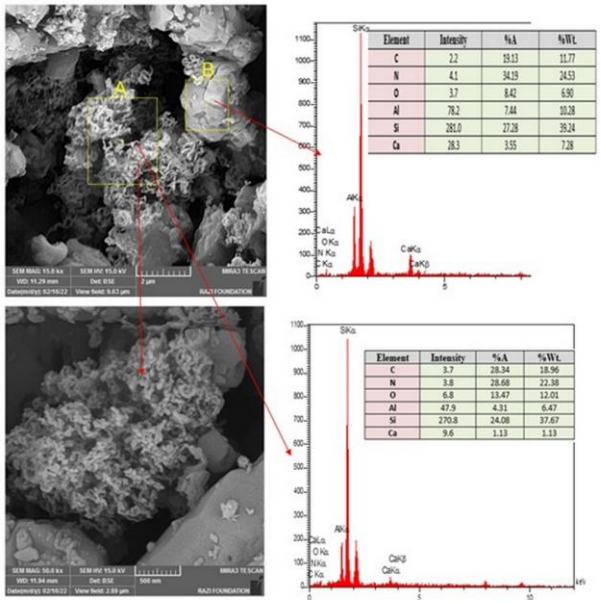

Figure 4. the morphology and chemical composition of the α-SiAlON powder prepared at 1500°C.

Two distinct types of oxynitride particles have formed in the obtained powder, exhibiting similar compositions but differing in particle size and morphology. The larger grains are micron-sized and irregularly shaped, while the other oxynitride compounds consist of nanoparticles smaller than 20 nm, which connect in specific directions. This suggests that different mechanisms may be involved in the development of these phases during the CRN process.

Figure 4 illustrates the morphology and chemical composition of the α-SiAlON powder prepared at 1500°C. The resulting α-SiAlON powder comprises nanometric particles smaller than 100 nm that connect and grow into elongated, wormlike structures in various directions. The presence of particles with different morphologies and similar compositions in the microscopic images of the attained SiAlON powders likely results from different synthesis mechanisms (O'Leary & MacKenzie, 2015).

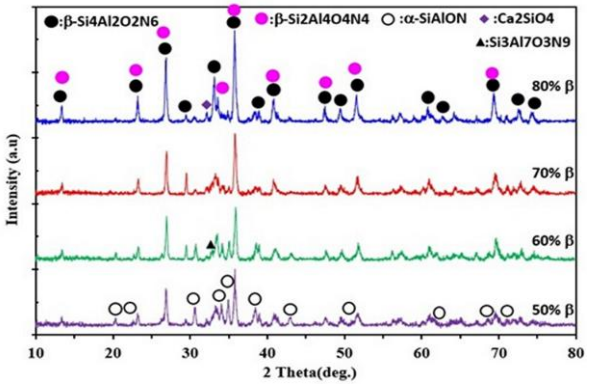

Figurer 5. XRD patterns of composites consolidated by spark plasma sintering (SPS) at 1800°C.

As shown in Figure 5, the main phases formed in all samples after spark plasma sintering (SPS) remained relatively unchanged. The primary SiAlON phases identified are β-$Si_4Al_2O_2N_6$ and α-$CaSi_9Al_3N_{15}$. Each composite exhibits varying proportions of β- and α-SiAlON phases, where the relative intensity of each phase is influenced by the initial mixing ratio of the synthesized components.

In the composite containing 80% β phase, the dominant phases are β-SiAlON in two forms: β-$Si_4Al_2O_2N_6$ and β-$Si_2Al_2O_2N_6$. Alongside these phases, α-SiAlON serves as a strengthening phase, while two compounds, Ca_2SiO_4 and $Si_3Al_7O_3N_9$, appear as impurities and secondary phases, respectively, in the microstructure after sintering. In composites containing 50% β phase, an increase in the α-SiAlON reinforcing phase leads to more pronounced peaks, reflecting a rise in their relative intensity.

All composites display a calcium silicate phase as an impurity, likely formed from the reaction between CaO—generated by the transformations and decomposition of α-SiAlON powder—and the SiO_2 present in the microstructure. The $Si_3Al_7O_3N_9$ composition is observed as a new phase in all composites except for the one with 80% β phase. Analysis of the peaks related to the β-SiAlON phase reveals that this phase is more stable than the α-SiAlON phase during the sintering process at high temperatures (1800°C), exhibiting fewer phase transformations.

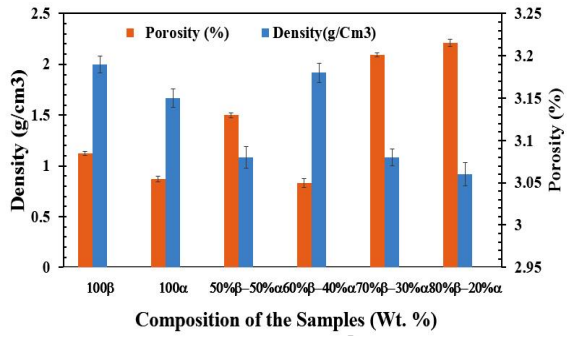

Figure 6. Effect of composition on the sintering behavior of the composites relative to pure SiAlON samples.

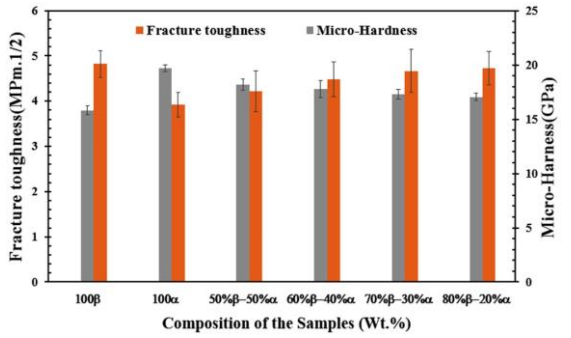

Figure 7. Influence of composition on the microhardness and fracture toughness of the composites compared to pure SiAlON samples.

To investigate the effect of composition on all produced samples, the density and porosity percentages of the sintered composites, along with their fracture toughness and microhardness, are presented in Figures 6 and 7. The data indicate that the synthesized α and β-SiAlON components, as well as the composites derived from them, achieve complete densification after being heated to 1800°C. This process results in a density exceeding 98% and a porosity below 2% for all samples produced in this study. These findings suggest that SiAlON powders synthesized from new precursors demonstrate excellent sintering capabilities.

Furthermore, as shown in Figures 4 and 5, the incorporation of the second component—synthesized α-SiAlON powder—into the β-SiAlON matrix results in a relative increase in hardness and a relative decrease in toughness compared to pure β-SiAlON samples. Figures 6 and 7 indicate that composites containing 50% β phase exhibit the highest hardness (18.22 MPa) and the lowest toughness (4.22 MPa.m$^{1/2}$). In contrast, composites containing 70% β phase achieve the highest density (3.18 g/cm^3) during sintering; however, they demonstrate lower microhardness and greater toughness compared to the composites with 50% β phase. The properties of composites produced using the new reagents in this study are comparable to those made from other materials (D. Liu et al., 2024; Nekouee & Khosroshahi, 2016).

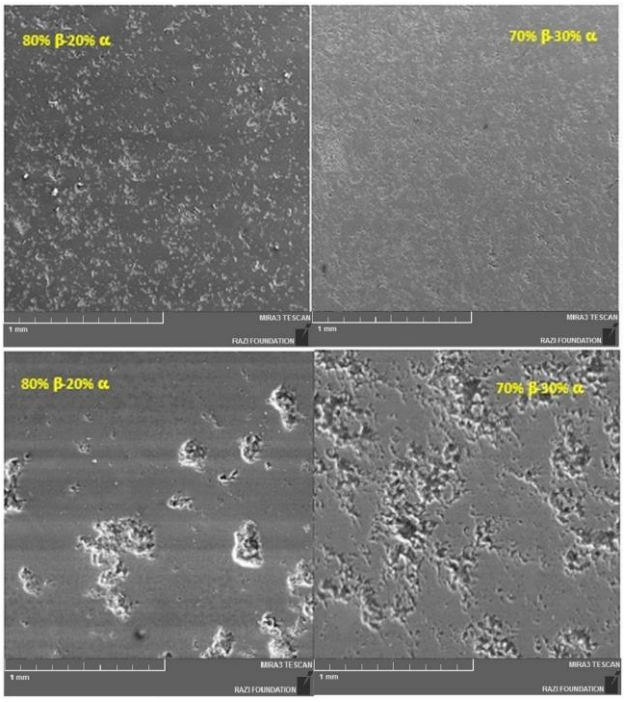

Figure 8. FSEM microscopic images showing two different magnifications of the composites containing 80% and 70% by weight of β-SiAlON.

Figures 6 and 7 indicate that the composites made with 50% β phase exhibit the highest hardness (18.22 MPa) and the lowest toughness (4.22 MPa.m$^{1/2}$).

The phases and their distribution were investigated using microscopic images of the microstructure of the samples. The images presented in Figure 8 reveal that, after the sintering process with Spark Plasma Sintering (SPS), dense composite bodies were formed, consistent with the results illustrated in Figure 6. The distribution of phases and the arrangement of elements in the cross-section of the composite containing 70% β-SiAlON and 30% α-SiAlON are depicted in Figures 9 and 10.

As shown in Figure 10, the composite contains elements such as Si, Al, O, N, and Ca. Some elements, like Si and Al, are predominantly and relatively homogeneously distributed in the matrix, while others, such as Ca—present in smaller quantities—are localized within specific regions of the microstructure. This distribution aligns with the compositional analysis of the SiAlON materials.

In Figure 10, the elemental analysis of the phases present in regions A, B, C, D, and E is shown. These results indicate that the phases formed in the microstructure contain not only the primary elements Si, Al, and O but also Ca and N, confirming the formation of SiAlON phases within the microstructure.

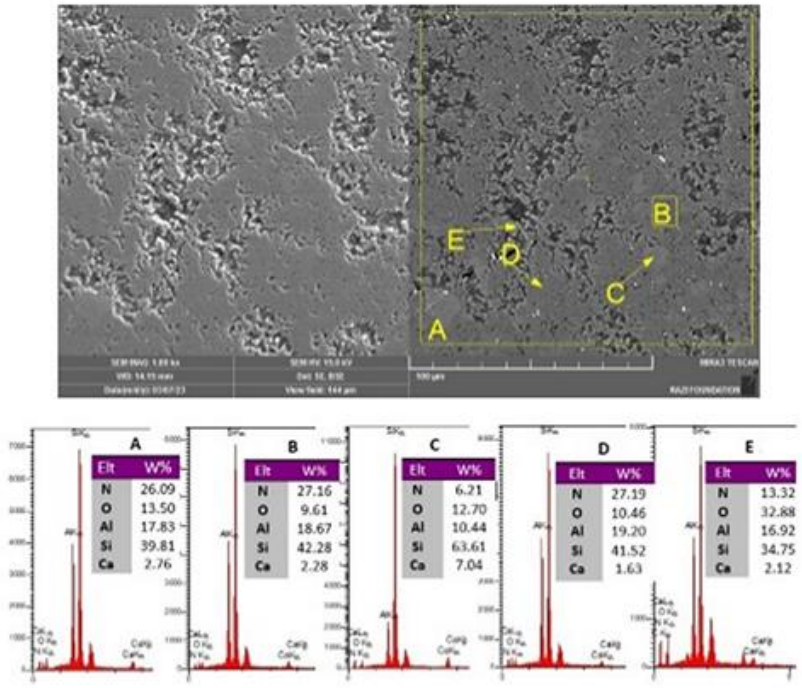

Figure 9. Distribution of elements in the cross-section of the composite containing 70% β-SiAlON-30% α-SiAlON.

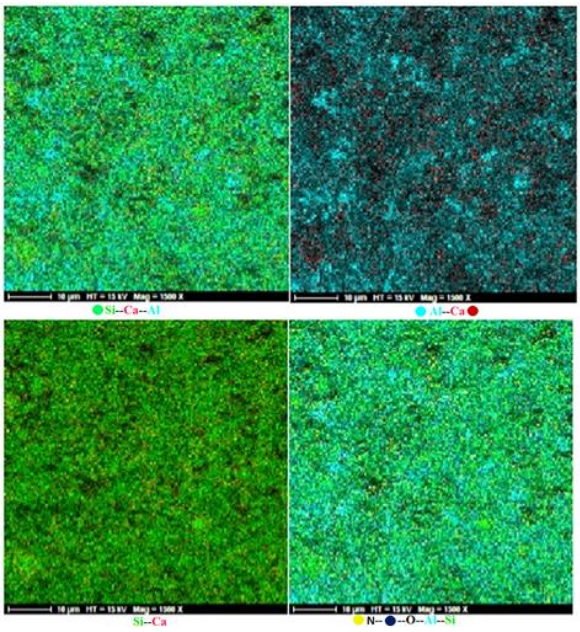

Figure 10. EDX analysis of the phases present in the microstructure of the composite containing 70% by weight of β-SiAlON after thermal and chemical etching at 485°C.

Regions A, B, and D, which are uniformly distributed throughout the sample, can be analytically interpreted as indicative of the presence of β- and α-SiAlON phases, as confirmed by the XRD analyses presented in Figure 4-1. Based on the elemental analysis shown in Figure 4-6, it appears that regions C and E contain impurity and secondary phases formed in the microstructure of the composite after the sintering process.

4. CONCLUSION(S)

The results of this research can be summarized as follows:

•Novel reagents were introduced for the mechanochemical synthesis of precursors essential for producing α and β-SiAlON phases.

•Fine and pure α and β-SiAlON powders were synthesized separately using a carbothermal reduction and simultaneous nitridation process at 1500°C.

•All composite samples densified easily during the Spark Plasma Sintering (SPS) process, achieving a high density of over 98%.

•A mixing ratio of 70% β-SiAlON powders to 30% α-SiAlON powders exhibited superior hardness, toughness, and favorable sintering properties compared to other ratios.

5. ACKNOWLEDGMENT

The authors would like to sincerely thank the staff of the Ceramic Laboratory, especially Mr. Ebrahim Jabari, Mr. Abbas Keshavarz, and Mr. Mohammad Ali Kabiri, for their exceptional contributions and support in carrying out various experiments.

REFERENCES

1. Abdi Maghsoudlou, M. S., Ebadzadeh, T. & Aghaei, A. (2022). Carbothermal synthesis, characterization, and mechanical properties of spark plasma sintered β-SiAlON (z = 2) powder prepared from mechanochemically activated precursors. Ceramics International, 48(23), 34243–34250. https://doi.org/10.1016/j.ceramint.2022.06.247
2. Antsiferov, V. N., Gilyov, V. G. & Karmanov, V. I. (2002). IR-spectra and phases structure of sialons. Vibrational Spectroscopy, 30(2), 169–173. https://doi.org/10.1016/S0924-2031(02)00022-X
3. Bagci, C., Hulbert, B. S., Yang, Q. & Kriven, W. M. (2023). Synthesis of SiAlON-type compounds by carbothermal reduction and nitridation of nanoparticulate geopolymers. Journal of the American Ceramic Society, 106(12),7375–7385. https://doi.org/10.1111/jace.19356
4. Basu, B., Vleugels, J., Kalin, M. & Van Der Biest, O. (2003). Friction and wear behaviour of SiAlON ceramics under fretting contacts. Materials Science and Engineering: A, 359(1), 228–236. https://doi.org/10.1016/S0921-5093(03)00349-6
5. Guo, F., Yin, Z., Chen, W., Liu, H., Hong, D. & Yuan, J. (2022). Spark plasma sintering of multi-cation doped (Yb, Sm) α/β-SiAlON ceramic tool materials: Effects of cation type, composition, and sintering temperature. Ceramics International, 48(22), 32730–32739. https://doi.org/10.1016/j.ceramint.2022.07.125
6. Jones, M. I., Hirao, K., Hyuga, H., Yamauchi, Y. & Kanzaki, S. (2003). Wear properties of Y–α/β composite sialon ceramics. Journal of the European Ceramic Society, 23(10), 1743–1750. https://doi.org/10.1016/S0955-2219(02)00401-6
7. Kheirandish, A. R., Nekouee, K. A., Khosroshahi, R. A. & Ehsani, N. (2016). Self-propagating high temperature synthesis of SiAlON. International Journal of Refractory Metals and Hard Materials, 55, 68–79. https://doi.org/10.1016/j.ijrmhm.2015.11.010
8. Kruzic, J. J., Satet, R. L., Hoffmann, M. J., Cannon, R. M. & Ritchie, R. O. (2008). The Utility of R-Curves for Understanding Fracture Toughness-Strength Relations in Bridging Ceramics. Journal of the American Ceramic Society,91(6),1986–1994. https://doi.org/10.1111/j.1551-2916.2008.02380.x
9. Kumar, R., Calis Acikbas, N., Kara, F., Mandal, H. & Basu, B. (2009). Microstructure–Mechanical Properties–Wear Resistance Relationship of SiAlON Ceramics. Metallurgical and Materials Transactions A, 40(10),2319–2332. https://doi.org/10.1007/s11661-009-9930-1
10. Liu, D., Yin, Z., Guo, F., Hong, D. & Yuan, J. (2024). Densification, microstructure and properties of α/β-SiAlON ceramic reinforced by SiC whiskers. Ceramics International, 50(21, PartB),42755–42765. https://doi.org/10.1016/j.ceramint.2024.08.121
11. Liu, L., Ye, F. & Zhou, Y. (2011). Microstructure and mechanical properties of the α-SiAlON/α-SiC composites: Effects of heat treatment. Ceramics International, 37(8), 3737–3741. https://doi.org/10.1016/j.ceramint.2011.05.001
12. MacKenzie, K. J. D. & Barneveld, D. Van. (2006). Carbothermal synthesis of β-sialon from mechanochemically activated precursors. Journal of the European Ceramic Society, 26(1), 209–215. https://doi.org/10.1016/j.jeurceramsoc.2004.10.004
13. McGarrity, K. A., Tumurugoti, P., Ning, K., George, C., Yan, Y., Wang, K. & Shulman, H. (2024). Exploration of an atomic-scale boron additive in SiAlON ceramics. International Journal of Ceramic Engineering & Science, 6(3),e10213. https://doi.org/10.1002/ces2.10213
14. Nag, A., Rao, R. R. & Panda, P. K. (2021). High temperature ceramic radomes (HTCR) – A review. Ceramics International, 47(15), 20793–20806. https://doi.org/10.1016/j.ceramint.2021.04.203
15. Nekouee, K. A. & Khosroshahi, R. A. (2016). Sintering behavior and mechanical properties of spark plasma sintered β–SiAlON/TiN nanocomposites. International Journal of Refractory Metals and Hard Materials, 61, 6–12. https://doi.org/10.1016/j.ijrmhm.2016.08.002
16. O'Leary, B. G. & MacKenzie, K. J. D. (2015). Inorganic polymers (geopolymers) as precursors for carbothermal reduction and nitridation (CRN) synthesis of SiAlON ceramics. Journal of the European Ceramic Society, 35(10), 2755–2764. https://doi.org/10.1016/j.jeurceramsoc.2015.03.026
17. Ogunbiyi, O., Jamiru, T., Adekoya, G. J. & Rominiyi, A. L. (2024). Structure-property relationship and emerging applications of nano- and micro-sized fillers reinforced sialon composites: a review. Journal of the Australian Ceramic Society, 60(4), 1167–1198. https://doi.org/10.1007/s41779-024-01020-y
18. Sopicka-Lizer, M., Duran, C., Gocmez, H., Pawlik, T., Mikuskiewicz, M. & MacKenzie, K. (2013). Effect of high energy milling on the formation and properties of sialon ceramics prepared from silicon nitride-aluminium nitride precursors. Ceramics International, 39(4), 4269–4279. https://doi.org/10.1016/j.ceramint.2012.11.006
19. Xu, X., Lao, X., Wu, J., Rao, Z., Zhou, Y., He, D. & Liu, Y. (2015). Preparation and Performance Study of Sialon-Si3N4-SiC Composite Ceramics for Concentrated Solar Power. International Journal of Applied Ceramic Technology, 12(5), 949–956. https://doi.org/10.1111/ijac.12374
20. Yi, H. C. & Moore, J. J. (1990). Self-propagating high-temperature (combustion) synthesis (SHS) of powder-compacted materials. Journal of Materials Science, 25(2), 1159–1168. https://doi.org/10.1007/BF00585421
21. Yi, X., Watanabe, K. & Akiyama, T. (2010). Fabrication of dense β-SiAlON by a combination of combustion synthesis (CS) and spark plasma sintering (SPS). RisIntermetallics, 18(4), 536–541. https://doi.org/10.1016/j.intermet.2009.10.004